Inorganica Chimica Acta 453 (2016) 330–338

Contents lists available at ScienceDirect

Inorganica Chimica Acta

journal homepage: www.elsevier.com/locate/ica

Research paper

Spectroscopic investigation of auranofin binding to zinc finger HIV-2 nucleocapsid peptides

Maria Antonietta Castiglione Morelli [a], Angela Ostuni [a], Giorgio Matassi [c], Camilla Minichino [a], Angela Flagiello [b], Pietro Pucci [b,d], Alfonso Bavoso [a,*]

[a] Department of Sciences, University of Basilicata, Potenza 85100, Italy
[b] CEINGE Advanced Biotechnologies s.c.a r.l., University of Napoli Federico II, 80100 Napoli, Italy
[c] Department of Agricultural, Food, Environmental and Animal Sciences, University of Udine, 33100 Udine, Italy
[d] Department of Chemical Sciences, University of Napoli Federico II, 80100 Napoli, Italy

ARTICLE INFO

Article history:
Received 8 June 2016
Received in revised form 6 August 2016
Accepted 8 August 2016
Available online 9 August 2016

Keywords:
Auranofin
Zinc finger
HIV-2
Mass spectrometry
CD
Fluorescence

ABSTRACT

The nucleocapsidic protein (NC) of orthoretroviruses has been considered as a promising target for antiretroviral drugs. Compounds, including zinc ejectors and metal derivatives capable to substitute the zinc ion in the nucleocapsidic zinc fingers, have been described. Auranofin, a gold(I) drug used for the treatment of rheumatoid arthritis, restricts the viral reservoir in the monkey AIDS model and induces containment of viral load following anti-retroviral therapy suspension. Here is reported a study of the interactions of auranofin with two synthetic CCHC-type peptides corresponding to the C-terminal zinc finger of the HIV-2 NC protein from two different isolates, using spectroscopic techniques and mass spectrometry. Both apopeptides interact very slowly with auranofin forming an Au-peptide complex. In contrast, as shown by mass spectrometry, the zinc-bound peptides interact on a shorter time-scale by forming an Et_3P-Au-peptide complex and an Au-peptide complex. The two peptides show kinetic differences in the formation of zinc complexes, in Zn^{2+} binding constants as well in Zn^{2+} displacement by Au^{+}.

1. Introduction

Lentiviruses constitute a genus of retroviridae family which includes several viruses (HIV-1, HIV2, SIV, Visna virus, FIV, EIAV, CAEV, BIV, etc.) infecting diverse species. They are host-specific viruses that cause slowly progressive diseases in their hosts.

The nucleocapsid proteins (NC) of orthoretroviruses are small (<100 amino acids), highly basic nucleic acid binding proteins containing either one (in Gammaretroviruses) or two (in all other *retroviral or Orthoretrovirinae* Subfamilies) strictly conserved zinc fingers with sequence C-X_2-C-X_4-H-X_4-C (CCHC). In all retroviral zinc finger proteins, the spacing of the zinc-binding residues is extremely conserved and so are the surrounding sequences within a particular retroviral species, as demonstrated, for instance, by various human immunodeficiency virus type-1 (HIV-1) and type-2 (HIV-2) sequences. Zinc finger proteins form stable structures with the NH_2- and COOH-terminal regions that are unstructured when the NC is not bound to nucleic acids [1].

In retroviruses, NC is synthesized as a functional domain of the Gag precursor. The mature NC is cleaved by a series of retroviral proteases during virus assembly in the infected cells. In orthoretroviruses, three main structural proteins are produced from Gag: matrix (MA), capsid (CA), and nucleocapsid (NC), as well as additional retrovirus-specific peptides. NC is required for viral replication, and genetic analyses have demonstrated that even minor mutations can affect the virus assembly step by disrupting either the genomic RNA packaging or the formation of infectious virus particles [2]. NC is a key component of virus assembly processes. It is responsible for binding to the RNA scaffold, thereby facilitating the interactions of other regions of Gag with one another and with cellular membranes, and it is required for the recognition and packaging of the RNA genome. Moreover, NC can cause defects in RNA dimer maturation, reverse transcription and integration [3]. Due to its key role in viral replication, NC has been indicated as a promising target for antiretroviral drugs and compounds, including zinc ejectors, targeting the retroviral HIV-1 NCp7 [4–6]. It has also been suggested that metal compounds could substitute the zinc

Abbreviations: Auranofin, 1-Thio-β-D-glucopyranosatotriethylphosphine gold-2,3,4,6-tetraacetate; TCEP, Tris(2-carboxyethyl)phosphine hydrochloride; PAR, 4-(pyridyl-2-azo)-resorcinol.

* Corresponding author.
E-mail address: alfonso.bavoso@unibas.it (A. Bavoso).

http://dx.doi.org/10.1016/j.ica.2016.08.012
0020-1693/

ion in the zinc fingers of NC, in particular gold and platinum derivatives [7,8].

Gold compounds (sodium aurothiomalate, aurothioglucose, auranofin) are thiol-reactive substances containing gold (I) (Au^{1+})-containing thiol-reactive substances used for the treatment of rheumatoid arthritis and other inflammatory disorders. The mode of action of these chemicals is due to reactions with cysteine (Cys) residues [9]. Gold (I) compounds alter gene expression, their anti-inflammatory activities likely involving interactions with Cys-dependent transcription factors [10,11]. In addition, it is known that gold fingers are formed when Au (I) interacts with Cys residues in zinc finger model peptides containing different CCCC, CCHH and CCHC motifs [12].

Auranofin is toxic towards parasites, cancer cells and leukemia cells [13], and is believed to act through the inhibition of different reduction/oxidation (redox) enzymes such as thioredoxin reductase [14,15], glutathione-S-transferase [16] and the zinc finger protein poly(adenosine diphosphate ribose)polymerase-1, PARP-1 [17]. Moreover, auranofin is known to restrict the viral reservoir in the monkey AIDS model and to induce containment of viral load following anti-retroviral therapy suspension [18].

In this study, we report the interactions of auranofin with the C-terminal zinc finger of the HIV-2 NC from two different isolates using spectroscopic techniques and mass spectrometry. The analysis of two divergent zinc finger CCHC peptides revealed the importance of the amino acid sequence effects in the interaction with auranofin and may help to clarify the antiviral activity of auranofin. To the best of our knowledge, this is the first study on the interaction of auranofin with CCHC zinc fingers.

2. Materials and methods

2.1. Phylogenetic analysis

Simian immunodeficiency viruses (SIV) and HIV-2 Gag sequences were retrieved from the Los Alamos National Laboratory (LANL) HIV sequences database (http://www.hiv.lanl.gov). Multiple sequence alignment was performed on amino acid sequences using MUSCLE [19]. PAL2NAL [20] was used to obtain the corresponding nucleotide alignment, which was subsequently edited in SeaView v. 4 [21]. The best model fitting the data was identified in jModelTest 2.1.7 [22]; the choice was based on a majority-rule consensus of the implemented statistics. Maximum likelihood phylogenetic inference was carried out on first and second codon positions under the TPM2uf + Γ4 (k = 010212) best-fitting model in PhyML v. 3 [23]. Tree-space was searched using the subtree pruning and regrafting (SPR) heuristic (BioNJ and five random starting trees). The aBayes statistic was used to assess branch support [24].

2.2. Samples

All reagents used in the present study were reagent grade and used without further purification. Apopeptides were produced by Fmoc-solid-phase peptide synthesis technology (Inbios srl, Naples, Italy) and correspond to residues 23–49 of HIV-2 NCp8 of two different isolates: respectively, peptide A (RAPRRQGCWKCGKPGHIMTNCPDRQAG) corresponds to isolate ROD (country Senegal, subtype A, GenBank accession M15390) and peptide H (KAPRRQGCWKCEKPGHNMASCPETKVG) to isolate 96FR12034 (country France, subtype U (formerly group H), GenBank accession AY530889). As received, the synthetic peptides had purity higher than 98%; the MALDI molecular masses given by the supplier were 3024.5 for peptide A and 2999.5 for peptide H, respectively. Auranofin (1-Thio-β-D-glucopyranosatotriethylphosphine gold-2,3,4,6-tetraacetate, purity ⩾98%), TCEP (Tris(2-carboxyethyl)phosphine hydrochloride, purity ⩾98%) and PAR (4-(pyridyl-2-azo)-resorcinol, purity ⩾95%) were purchased from Sigma-Aldrich (Scheme 1).

2.3. Circular dichroism spectroscopy

Circular dichroism (CD) spectra were recorded on a Jasco J-600 spectropolarimeter using a 0.1 cm path-length cylindrical quartz cell. Peptide samples at 58.3 μM concentration in a 10 mM sodium phosphate buffer at pH 7.2 were reduced with TCEP (peptide:TCEP ratio = 1:3.6). $ZnCl_2$ was dissolved in water at concentration of 50 mM and added to peptides (peptide:$ZnCl_2$ ratio = 1:1.2) 30 min before recording spectra. Auranofin was dissolved in methanol at concentration of 6.5 mM and added to peptides (peptide:auranofin ratio = 1:1.2). Data were acquired at 20 °C and were baseline corrected by subtraction of buffer/TCEP or buffer/TCEP/$ZnCl_2$ or buffer/TCEP/auranofin. In each case, the final spectrum is the sum of 16 separate spectra with a step resolution of 0.1 nm, a 2-s time constant, a 50 nm min^{-1} scan speed, a 1 nm bandwidth and a 20 mdg sensitivity.

2.4. UV–vis spectroscopy

The solutions containing PAR (25 μM), $ZnCl_2$ (7.5 μM) and reduced peptides (58.3 μM) were prepared and used to record absorption spectra in the range 350–600 nm using a CARY-5E-Spectrophotometer. Identical conditions were adopted when auranofin (to a final concentration of 12 μM) was added to PAR-peptide-Zn complexes. The experiments were performed at 20 °C.

2.5. Intrinsic fluorescence measurements

The intrinsic tryptophan fluorescence of reduced peptides (3 μM) was measured in sodium phosphate buffer (10 mM, pH 7.2) alone or in the presence of $ZnCl_2$ (peptide:$ZnCl_2$ ratio = 1:1.2) or auranofin (peptide:auranofin ratio = 1:1.2). The experiments were performed at 20 °C with a thermostated Agilent Technologies Cary Eclipse Fluorescence Spectrophotometer. The excitation wavelength was set at 295 nm and emission was scanned over the range 300–450 nm, with scan rate of 30 nm/min, averaging time 1 s and data interval 0.5 nm.

The method employed by Mély et al. was used for the determination of the Zn^{2+} binding constants where the metal complexant EDTA was used "to buffer very low free Zn^{2+} concentrations" [25]. Fluorimetric titrations were performed by adding increasing concentrations of zinc chloride to a given peptide in the presence of 1 mM EDTA. After each addition of 1 μl of $ZnCl_2$ 5 mM, the fluorescence intensity change was monitored at the maximum emission wavelength (~353 nm) for at least 15 min to ensure that equilibrium was reached. From the fluorimetric titrations the average number ν of Zn^{2+} moles bound per peptide mole was evaluated by $\nu = (I - I_0)/(I_t - I_0)$, where I is the fluorescence measured after each zinc addition, I_0 the fluorescence of the apopeptide and I_t that

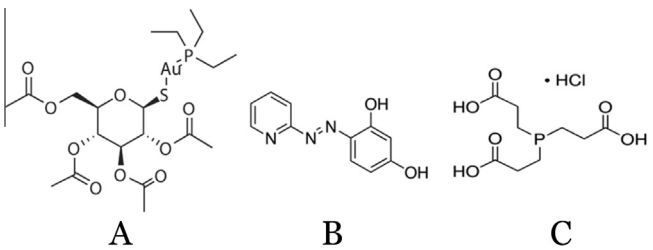

Scheme 1. Chemical structures of: A) auranofin; B) PAR and C) TCEP.

of the fully saturated peptide [25,26]. The binding constants are the results of at least three independent determinations performed under the same experimental conditions.

2.6. Mass spectrometry analyses

An aliquot of auranofin, previously dissolved in methanol to a final concentration of 6.5 mM was directly submitted to MALDI-MS analysis.

Each peptide was dissolved in ammonium acetate (5 mM, pH 7) to a final concentration of 300 μM.

Auranofin-peptide complexes were prepared by incubation of auranofin with each peptide solution to a peptide:auranofin molar ratio of 1:1.2. Prior to auranofin addition, the non-thiol reducing agent TCEP was added to each peptide solution to a molar ratio peptide:TCEP of 1:3.6 in order to prevent oxidation of cysteine residues. The ESI-MS analysis was carried out on a time course basis by recording spectra at different incubation times (0 h, 24 h, 48 h, 1 week and 1 month).

In order to study the displacement of the zinc ion from the peptides upon addition of the auranofin to the peptide-TCEP mixture, an aliquot of $ZnCl_2$, previously dissolved in H_2O to a final concentration of 100 mM, was added to a molar ratio peptide:Zn of 1:1.2. Aliquots of the peptide-Zn complexes were submitted to ESI-MS analysis after 1 h of incubation. Afterwards, an aliquot of auranofin was added to peptide-TCEP-$ZnCl_2$ mixture (final molar ratio peptide:auranofin = 1:1.2) and aliquots of the complexes were submitted to ESI-MS analysis at different incubation times (10 min, 1 h, 24 h, 4 days, 1 week, 2 weeks and 3 weeks).

MALDI-MS analyses were carried out on a 4800 plus MALDI TOF-TOF Analyzer mass spectrometer (AB Sciex) equipped with a reflectron analyser and used in delayed extraction mode with 4000 Series Explorer v3.5 software. Aliquot of 0.5 μl of the sample was mixed with an equal volume of α-cyano-4-hydroxycynnamic acid as matrix (10 mg/ml in 0.2% TFA in 70% acetonitrile), applied to the metallic sample plate and air dried. Mass calibration was performed by using the standard mixture provided by manufacturer. MALDI-MS spectra were acquired over a mass range of 600–5000 m/z in the positive-ion reflector mode. MS spectra were acquired and elaborated using the software provided by the manufacturer.

ESI-MS analyses were performed on a Quattro micro mass spectrometer (Waters) equipped with a triple quadrupole and an electrospray source. Sample solutions were introduced into the electrospray ion source by a syringe pump. Calibration was performed using multiply charged ions from a separate introduction of horse heart myoglobin. Spectra were acquired in a mass range of 500–1200 m/z and elaborated using the software provided by the manufacturer. Molecular masses are given as average values.

2.7. NMR spectroscopy

Peptides were dissolved in 10 mM sodium phosphate buffer-20% D_2O (pH 7.2) to give a final concentration of approximately 1 mM peptide. TCEP was added to prevent the oxidation of the cysteine residues (peptide:TCEP ratio = 1:3.6). 1.2 equivalents of $ZnCl_2$ were then added to form the complexes.

The auranofin-peptide complexes were prepared by dissolving the peptide in 10 mM sodium phosphate buffer-20% D_2O (pH 7.2) with TCEP and then adding auranofin in slight excess (1.2 equivalents) with respect to peptide concentration.

^1H NMR data were collected using a VARIAN Unity Inova 500 MHz spectrometer with sample at 298 K. Chemical shifts were referenced to the methyl resonance signal of TSP (3-(trimethylsilyl)propanoic acid) used as internal standard.

2D TOCSY, ROESY and NOESY experiments were recorded in phase sensitive mode using different mixing times (65 and 80 ms for TOCSY; 200, 300 and 400 ms for ROESY; 100, 150 and 250 ms for NOESY experiments). The number of transients were 32 for both TOCSY and ROESY with 256 experiments; in NOESY experiments 64 transients were acquired for 512 experiments. The spectral width was 5989 Hz in both dimensions. In all the experiments the water signal was suppressed by presaturation or with a *dpfgse* pulse sequence.

3. Results

3.1. Choice of the peptides for spectroscopic studies

Both HIV-1 and HIV-2 exhibit considerable genetic variation, which consequently has been used to classify isolates into genetic subtypes, formerly defined as groups, designated A to G. In the LANL HIV Sequence Database the majority of HIV-2 sequences belong to subtypes A and B. Compared to HIV-1, only a small number of HIV-2 complete genomes have been determined (http://www.hiv.lanl.gov/).

Two strategies were used to select the peptides: (i) the phylogenetic analysis of the genes coding for the Gag protein, and (ii) the sequence divergence at the amino acid level with respect to the C-terminal zinc finger of NCp8.

Molecular phylogenetic analysis was carried out on a dataset of 27 HIV-2 Gag-polyprotein and 16 SIV Gag homologs. Maximum likelihood inference was carried out on first and second codon positions under the best-fitting evolutionary model (see Section 2 and Fig. S1, Supplementary information). Two sequences were selected: peptide A (GenBank accession M15390) in the HIV-2 subtype A clade, which comprised also NCp8, and peptide H (GenBank accession AY530889) belonging to the divergent subtype U. As to sequence divergence, peptide A and H differ at 5 and 8 amino acid residues, respectively, compared to the NCp8 sequence (GenBank accession M30895) studied by Matsui et al. [27] (Fig. 1). Peptide A belongs to the most infectious and diffuse subtype A, whereas peptide H belongs to the subtype U and was identified in France from a patient of West African origin, formerly defined as lineage H [28].

3.2. CD analysis of the zinc finger peptides

The effects of Zn^{2+} and Au^{+} on secondary structures of peptide A (Fig. 2A) and peptide H (Fig. 2B) were investigated by CD spectroscopy. CD spectra were recorded for apopeptide, peptide-Zn complex (immediately and after 2 h) and peptide-auranofin complex (immediately, after 24 h and after 5 days).

CD spectra of the peptides in absence of zinc are compatible with random coil conformations. The spectra of both peptide-Zn complexes show a pronounced less negative ellipticity with respect to the free peptide with no shift of the minimum in the

	Sequences
NCp8	RAPRRQGCWKCGKTGHVMAKCPERQAG
Peptide A	RAPRRQGCWKCGK**P**GH**I**M**TN**CP**D**RQAG
Peptide H	**K**APRRQGCWKC**E**K**P**GH**N**MA**S**CPE**TKV**G

Fig. 1. Primary structures of peptide A (GenBank accession M15390) and peptide H (GenBank accession AY530889). In boldface and underlined are represented residues different from the (23–49) HIV-2 NCp8 sequence studied by Matsui et al. (GenBank Accession number M30895) [27].

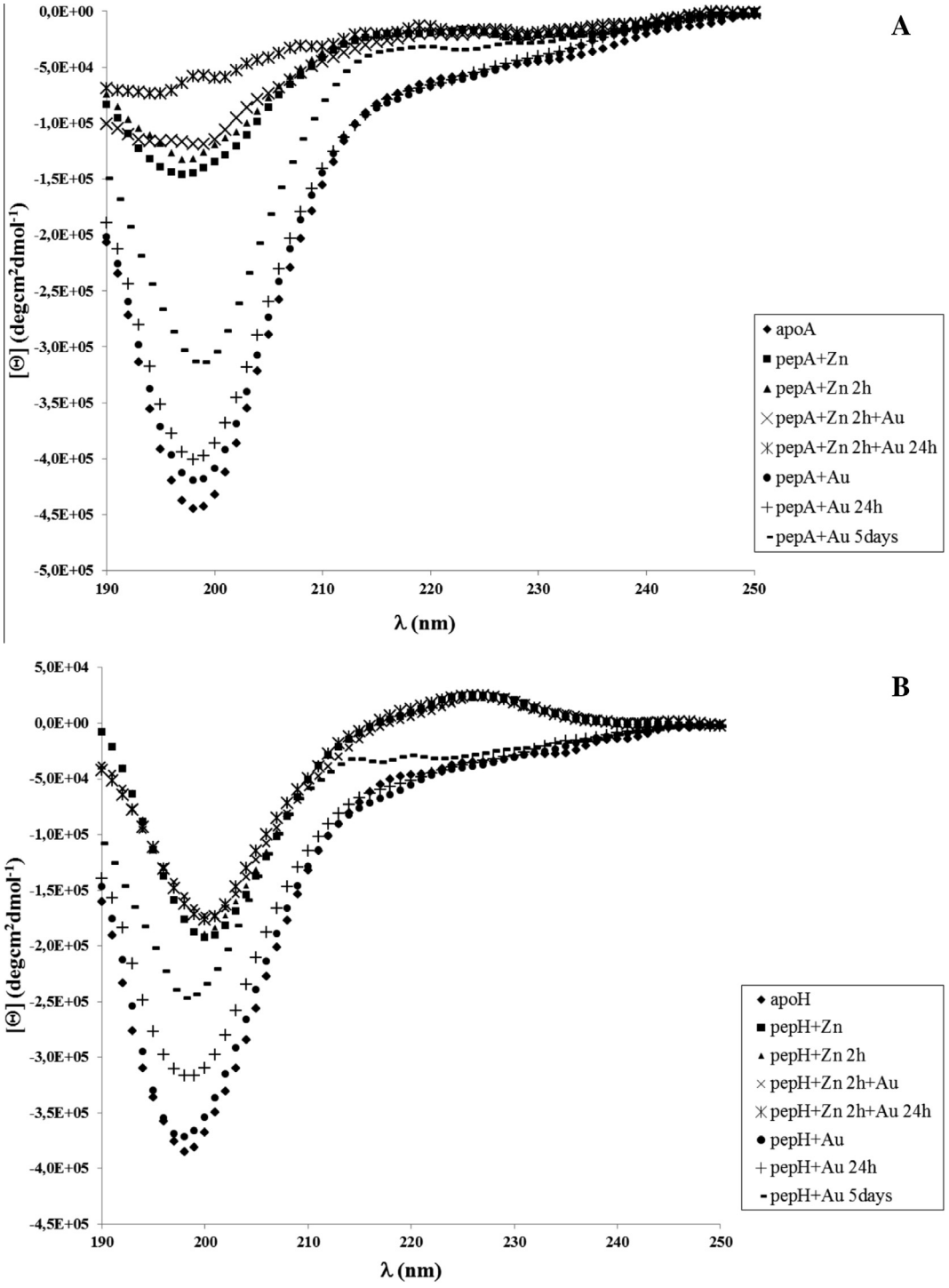

Fig. 2. A) CD spectra of peptide A: apopeptide (◆); peptide plus Zn^{2+} immediately (■), after 2 h (▲), plus auranofin immediately (x) and after 24 h (⁎); peptide plus auranofin immediately (●), after 24 h (+) and after 5 days (-). B) The same measurements were performed also on peptide H. The data were expressed in terms of the molar ellipticity.

spectrum of peptide A, while there is but a 2-nm red shift of the minimum in the spectrum of peptide H.

These findings indicate that the structures are more ordered in presence of zinc. Much less substantial secondary structure change was observed for both peptides in the presence of auranofin.

Lastly, the effect of auranofin on the peptide-Zn complexes was monitored. This led to a change in spectrum of peptide A, but no substantial change was observed in the spectrum of peptide H. This could be indicative of an overall modification of the zinc finger structure of peptide A due to Au(I) binding.

3.3. UV–visible spectroscopic investigation

We used PAR to qualitatively confirm zinc ejection from the CCHC nucleocapsid zinc finger [8]. PAR is a tridentate ligand forming ML_2 type complexes with Zn(II) and other transition metals and is used to measure micromolar concentrations of these metals [29]. Free PAR absorbs at ~410 nm whereas the PAR_2-Zn complex shows an absorption maximum at ~500 nm. The most important physicochemical parameters of this highly used chromogenic chelator have been recently updated [30].

In order to verify that auranofin does not interact with PAR and that it is not able to displace zinc from PAR, preliminary tests were carried out at the same experimental conditions used in presence of peptides: no interference was observed in the PAR_2-Zn absorption spectrum due to auranofin and/or TCEP.

We next assessed the metal binding properties of both peptides by displacing zinc from PAR in competition assays. Peptide H was able to displace zinc ions from the PAR_2-Zn complex although to a lesser extent than EDTA. In fact, when added (peptide/$ZnCl_2$ ratio = 1:1.2) to a solution containing the PAR_2-Zn complex, peptide H lowered the absorbance maximum at 500 nm (Fig. 3B). Addition of auranofin (peptide/auranofin = 1:1.2 ratio) to a solution containing the peptide H-Zn complex and PAR, led to an increase of the PAR_2-Zn absorbance maximum. This indicates that auranofin is complexed with peptide H and therefore zinc is again accessible for forming the PAR_2-Zn complex. Thus, auranofin is able to displace zinc from peptide H-Zn complex, at least in these experimental conditions.

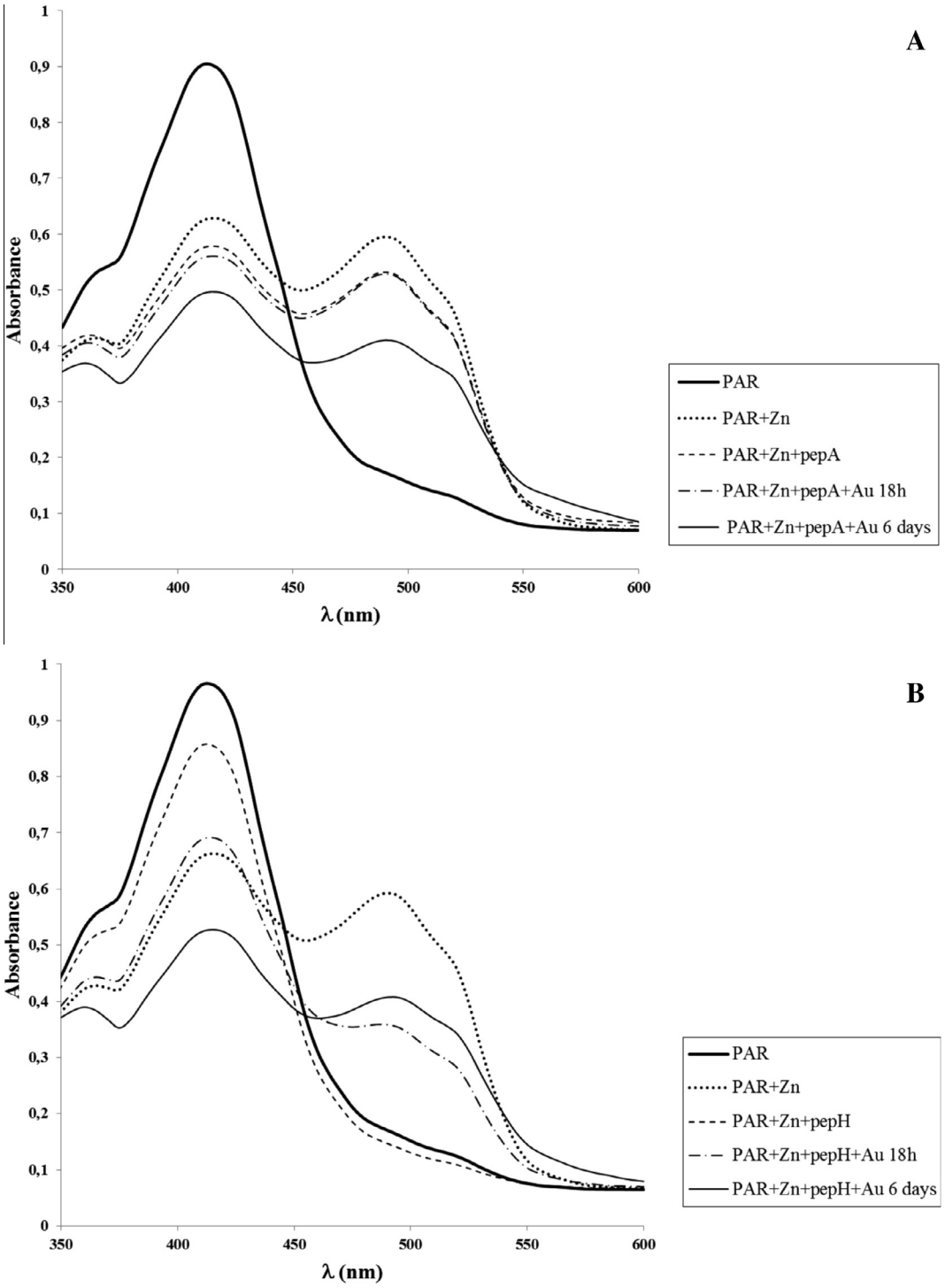

Fig. 3. A) Absorption spectrum of 25 μM PAR alone (–), with 7.5 μM Zn^{2+} (··) and 58.3 μM peptide A (- -) in phosphate buffer pH 7.2 at 25 °C. Spectra were also taken at 18 h (-·-) and 6 days (–) after the addition of auranofin. B) The same measurements were performed also on peptide H.

Conversely, the complex peptide A-Zn apparently does not form when PAR is present, therefore auranofin seems not to be active (Fig. 3A). Indeed, the absorbance-maximum at ~500 nm was not modified. Noteworthy, the spectra of peptides A and H, after an incubation time of 6 days with auranofin (Figs. 3A, B and S2), are nearly identical. This finding seems to indicate that, as described for peptide H, similar mechanisms of complex formation and displacement could be also valid for peptide A, although with different kinetics.

3.4. Fluorescence spectroscopy investigation

To monitor the binding of zinc to peptides we used the fluorescence of the single naturally occurring tryptophan (Trp) at position 31. The fluorescence increases upon addition of Zn(II) and the maximum emission wavelength shifts from 351 to 338 nm (Fig. 4). This blue-shifted emission is typical of Trp residues in apolar environments while protein unfolding leads almost always to a red shift [31].

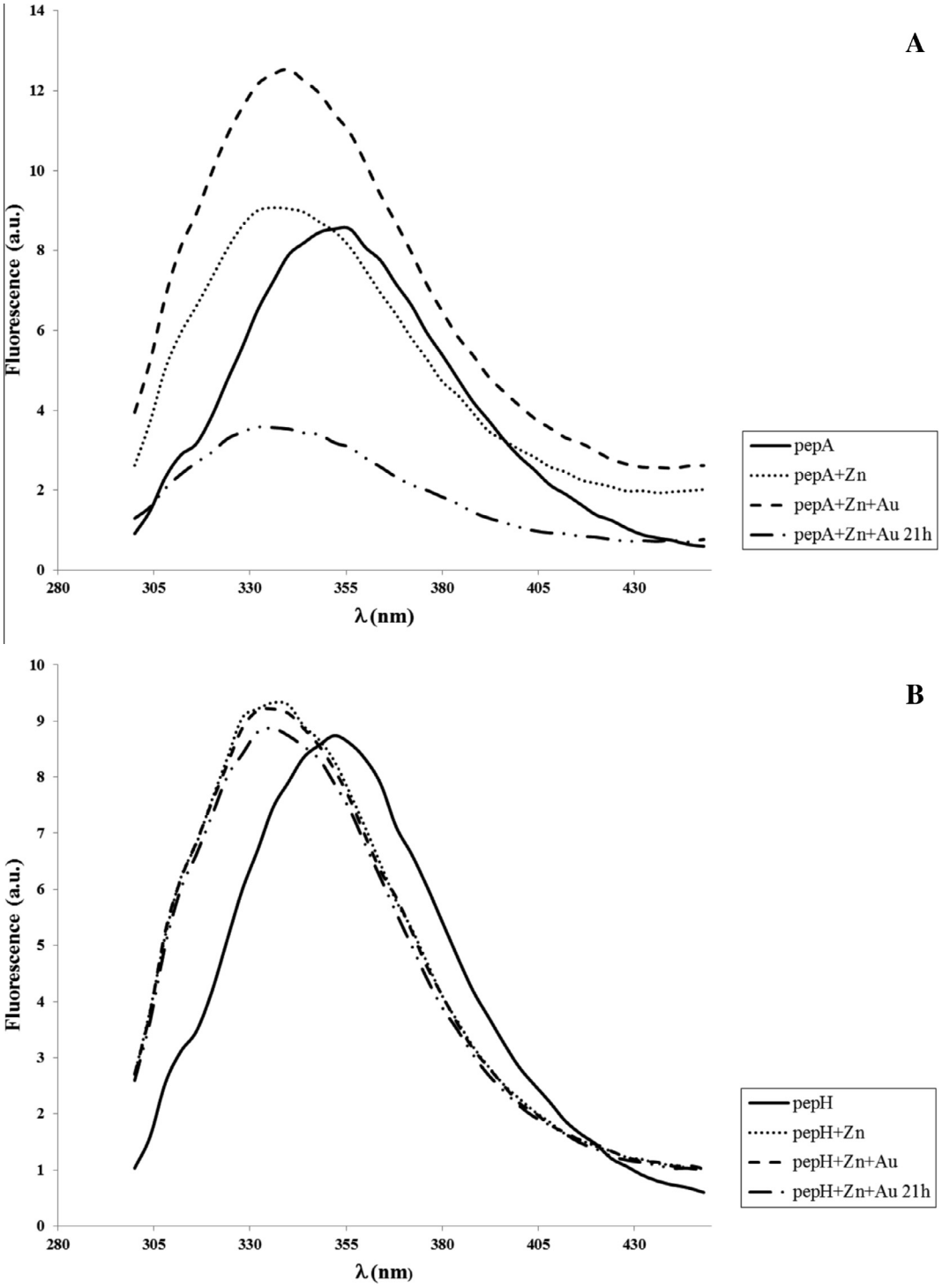

Fig. 4. Intrinsic fluorescence spectra (λexc = 295 nm) of: A) peptide A and B) peptide H in the absence (–) and presence of Zn (II) (..) and auranofin immediately (- -) and after 21 h (-.).

The method employed by Mély et al. [25] was used for the evaluation of the Zn^{2+} binding constants. The fluorescence quantum yields of both peptide A and peptide H were observed to increase linearly with sub-stoichiometric additions of zinc (data not shown). At pH 7.2 the conditional zinc binding constants of peptide A and peptide H were $5.94 \pm 0.85 \times 10^{14}\ M^{-1}$ and $8.61 \pm 0.61 \times 10^{14}\ M^{-1}$, respectively. These constants support the qualitative data obtained by absorption spectroscopy of different zinc binding of peptide H in comparison with peptide A (see above).

Furthermore, the intrinsic fluorescence of Trp^{31} was also used to assess qualitatively the susceptibility of the Zn(II)-peptide complexes to Au(I) presence. The addition of auranofin has a marked effect on peptide A where the fluorescence intensity sharply increases (by about 1.5-fold) and decreases noticeably after 21 h (by about 2.3-fold) (Fig. 4A). In contrast, for peptide H no fluorescence change is observed after auranofin addition (Fig. 4B). This finding is indicative of no significant variation of Trp^{31} environment and suggests a tighter binding of Zn to peptide H.

3.5. NMR study

Preliminary ^1H NMR studies were performed on peptide A and peptide H. Both apopeptides were unstructured in phosphate buffer at pH 7.2, whereas the formation of the zinc finger induces

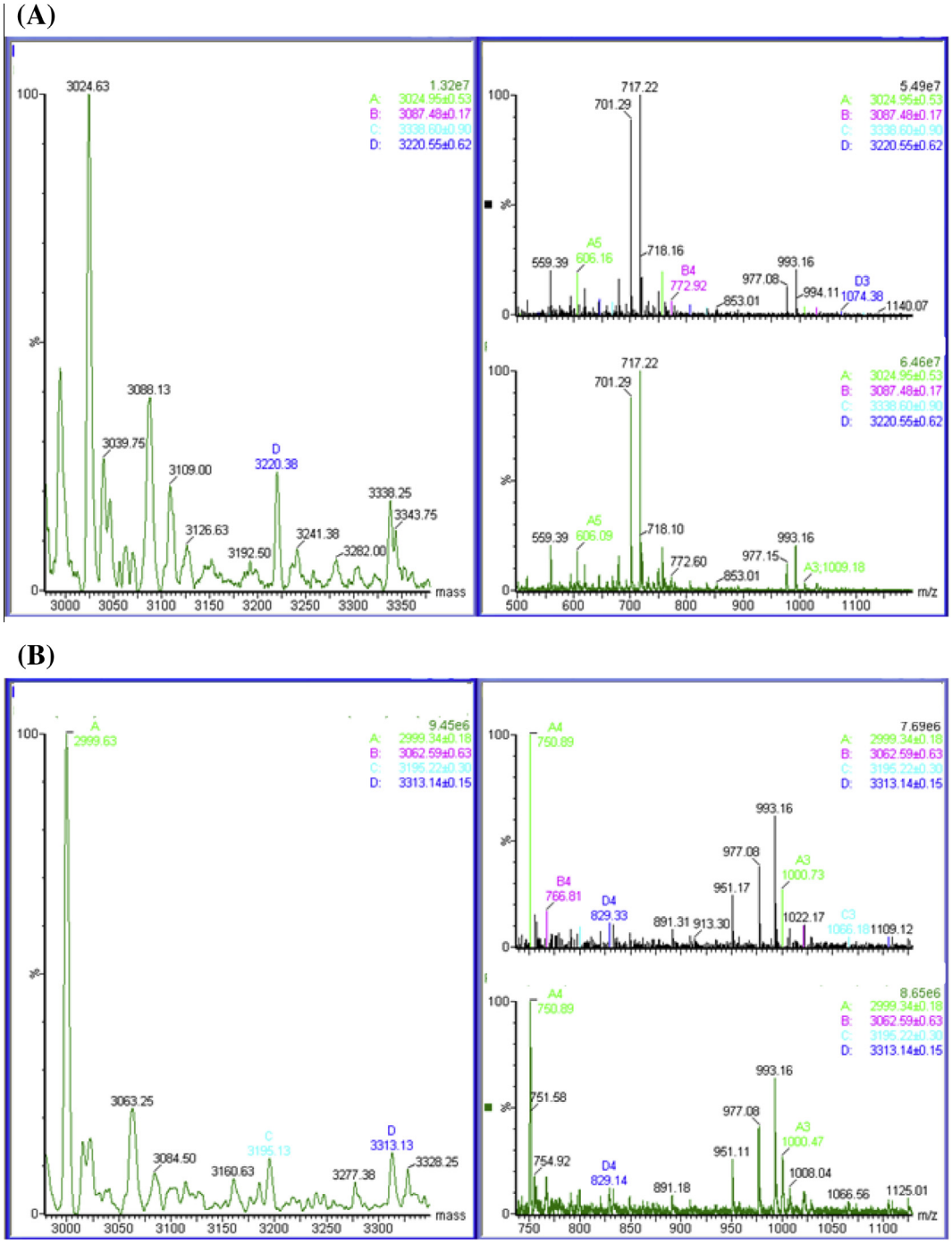

Fig. 5. ESI MS spectra of: (A) peptide A and (B) peptide H (300 μM peptide in 5 mM ammonium acetate (pH = 7), $ZnCl_2$ (molar ratio peptide:$ZnCl_2$ = 1:1.2) after 1 h incubation time with auranofin (molar ratio peptide/auranofin = 1:1.2). The MW values of all species were calculated from +4 and +3 charged ions indicated by labels in the right panels of the figure.

peptide folding, as evidenced by a better dispersion of the resonances in the spectra and good quality 2D-NMR spectra (Figs. S3 and S4). For both peptides we recorded also spectra in presence of auranofin. The 1D-NMR spectra of the peptides recorded 24 h after the addition of auranofin resemble those of the apopeptides. In addition, the absence of significant NOEs in NOESY and ROESY spectra recorded at different times after auranofin addition precluded further structural characterization of the gold complexes by NMR (data not shown).

3.6. Mass spectrometry

ESI-MS spectrometric analysis was used to gain additional evidence on the interaction of peptide A and peptide H with auranofin. First, an aliquot of auranofin, 6.5 mM in methanol, was analysed by MALDI mass spectrometry (Fig. S5). The observed molecular mass at *m*/*z* 993.1 is due to an auranofin molecule bound to an Au-P(CH_2CH_3)$_3$ group, probably via the sulfur atom. The molecular ion at *m*/*z* 1553.1 was attributed to an adduct formed by two auranofin molecules bound via an additional Au^+ ion that eventually links the sulfur atoms of the auranofin molecules (Au-Au bonds should be considered). Finally, the two mass ions at *m*/*z* 977.1 and 1537.1 displayed a mass difference of 16 Da from signals at *m*/*z* 993.1 and 1553.1, respectively; this discrepancy may be accounted for by a possible presence of trace impurity in the commercial sample.

The formation of the peptide-auranofin complexes was investigated by ESI-MS analyses. Auranofin was added to the apopeptide solutions in the presence of the non-thiol reducing agent TCEP. ESI-MS analysis was carried out on a time course basis by recording spectra at different incubation times (0 h, 24 h, 48 h, 1 week and 1 month). Fig. S6 shows the results obtained after one month incubation time for peptide A and peptide H. Mass signals at *m*/*z* 3220.3 and 3194.3 were assigned to the peptide A and peptide H complexed with Au^+, respectively. This may be due to the Au^+ ion binding to the first two cysteines of the peptide; however, the other two isomers cannot be excluded. These complexes were not observed at shorter incubation times, in the range 1–7 days.

MS was also used to study the displacement of the zinc ion from the zinc finger peptides upon addition of auranofin. The ESI-MS spectrum of peptide A, after one hour from the addition of the zinc ion, shows a mass signal at *m*/*z* 3087.2 corresponding to the peptide complexed to zinc (Fig. S7A). A corresponding complex displaying molecular mass of 3062.7 was observed in the case of peptide H (Fig. S7B). Auranofin was then added to both peptide complexes and the ESI-MS spectra were recorded at different incubation times in the range 10 min–3 weeks. In the case of the zinc finger of peptide A, after one hour of incubation with auranofin the ESI-MS spectra demonstrated the presence of the reduced peptide A (MWav: 3024.9), the peptide-zinc ion complex (MWav: 3087.5), the peptide-Au^+ complex (MWav: 3220.6) and the peptide-Au-triethylphosphine complex (MWav: 3338.6) (Fig. 5A). The corresponding species were also observed in the case of the zinc finger of peptide H after one hour of incubation with average masses of 2999.3, 3062.6, 3195.2 and 3313.1, respectively (Fig. 5B). The peaks corresponding to all the above mentioned peptide species were observed in all the ESI-MS spectra taken after incubation times of 24 h, 4 days, 1 week, 2 weeks and 3 weeks for peptide A (Figs. S8A–S12A). In the case of peptide H, all the species were also observed in the spectrum registered after 24 h of incubation. On the contrary, the molecular mass corresponding to the peptide H-Au-triethylphosphine complex was never found in the ESI-MS spectra measured after 4 days, 1 week, 2 weeks and 3 weeks (Figs. S8B–S12B).

Two conclusions can be drawn. First, the complexes of the two peptides with gold are initially observed at considerably shorter times when the zinc ions are present, suggesting a possible "catalytic" role of the zinc ions. Second, the peptides show different binding characteristics, since the peptide-Au-triethylphosphine complex is always found in peptide A but not in peptide H.

4. Discussion

Auranofin has been used in the treatment of rheumatoid arthritis and psoriatic arthritis. In this context, Shapiro and Masci [32] observed that an HIV-1 patient treated with auranofin for psoriatic arthritis, but not with anti-retroviral therapy, showed a significant increase in $CD4^+$ lymphocyte count, thus suggesting that auranofin had caused the improvement in the patient's conditions. Recently, it has also been found that a combined anti-retroviral and auranofin therapy in rhesus macaques infected with a HIV simian homolog, is able to maintain a reduced viral titre long-term after treatment withdrawn [18]. Noteworthy, other aurothiolates derivatives of gold (I) (aurothioglucose and aurothiomalate) inhibit the HIV-1 infectivity *in vitro* by activating gold(I) ligand exchange between the reactive species bis(thiolate) gold(I) and acidic thiol groups exposed on the surface of virion proteins [33]. A different mechanism has been recently proposed, whereby auranofin could target the infected cells (T-lymphocytes) through the inhibition of reduction/oxidation (redox) enzymes such as thioredoxin reductase and subsequent induction of cell apoptosis [34].

Our results suggest that auranofin, and eventually other aurothiolate drugs, could also modulate and/or inhibit the HIV nucleocapsidic protein. The mechanism of coordination and zinc ejection from NC due to aurothiolate drugs (gold(I)) could be the same described in a study of the interactions of Gold(I)-Phosphine-N-Heterocycle compounds with the C-terminal HIVNCp7 zinc finger [7].

ESI-MS analyses have unequivocally shown that: (i) peptide complexes with Au are formed slowly when the apopeptides are allowed to react with auranofin (Fig. S6); (ii) the formation of complexes is fast when the zinc-bound peptides are used. In fact, we observed an Et_3P-Au-peptide complex in a first reaction step with both the studied peptides and an Au-peptide complex produced in a second reaction step via displacement of PEt_3 (Fig. 5). However, we have no evidence of an Au_2-peptide complex, as reported in the previously cited investigation [7]. The chemistry of gold(I) complexes is dominated by linear two-coordinate complexes of the form *ligand*$_1$-Au-*ligand*$_2$ [35]. In our case a complex is formed with two cysteines but we cannot distinguish between the possible different isomers due to the presence of three cysteines. Therefore, we cannot ascertain if we are dealing with a single isomer or a mixture. In addition, different isomers could be formed depending on the specific experimental conditions.

Possible reasons of the slower reactivity of the apopeptides could be both the absence of a structural preorganization induced by zinc binding and the protonation state of the cysteines. In the apopeptides cysteines are predominantly in the thiol form, whereas in the zinc finger the thiolate form is likely present [36,37]. According to the Hard/Soft Acid/Base (HSAB) theory, sulfur is a relatively soft and polarizable atom; Au^+ and Zn^{2+} are a soft and a borderline ion, respectively [38]. Upon ionization of the thiol (i.e., $SH \rightarrow S^-$), the consequent expansion of the anionic cloud increases the softness and yields the easily polarizable thiolate nucleophile. Consequently, the soft electrophile Et_3PAu^+ competes favorably with the Zn^{2+} ions for the thiolate and the exchange occurs. The Zn-bound thiolates of the zinc fingers have been reported to have different susceptibility to electrophilic attack that depend on the specific Cys residue [39,40].

These characteristics, together with conformational sequence-related peculiarities, may lead to differences in the complexation properties of the zinc finger peptides with zinc or other metals.

In the MS experiments we observe the same type of complexes for peptides A and H, but some differences were found. The most significant one is the disappearance of the peptide H-Au-triethylphosphine signal after 4 days of incubation with the drug, while peptide A shows the corresponding signal for the entire time-span investigated.

The results of the spectroscopic investigations are less straightforward to interpret. In CD spectra of peptide H no substantial change in the zinc finger structure is observed upon auranofin addition (Fig. 2B); besides, for zinc-bound peptide H no change was noticed in fluorescence spectra when auranofin is added (Fig. 4B). Furthermore, absorption spectroscopy data in presence of PAR indicate that peptide H forms readily a zinc complex by displacement of Zn^{2+} from PAR and that Au^{+} is able to displace quickly Zn^{2+} (Fig. 3B). On the contrary, zinc-bound peptide A interacts with Au^{+} on a short time-scale as evidenced by the marked effect both in CD (Fig. 2A) and in fluorescence spectra (Fig. 4A) upon auranofin addition. However, in presence of PAR, peptide A binds slowly to Zn^{2+} and Au^{+} is apparently able to displace Zn^{2+} (Fig. 3A).

Taken together, our results indicate that the peptide-zinc complexes from two different isolates of HIV-2, in appropriate conditions, can react with the drug auranofin by forming gold complexes, while the apopeptides form gold complexes as well, but slowly. In addition, our results show that the reactivity of the zinc finger towards auranofin can be influenced by the specific amino acid sequence. Therefore, we suggest that the HIV nucleocapsidic protein could be considered as a potential target of auranofin.

Appendix A. Supplementary data

Supplementary data associated with this article can be found, in the online version, at http://dx.doi.org/10.1016/j.ica.2016.08.012.

References

[1] P. Amodeo, M.A. Castiglione Morelli, A. Ostuni, G. Battistuzzi, A. Bavoso, Biochemistry 45 (2006) 5517–5526.
[2] D. Muriaux, J.L. Darlix, RNA Biol. 7 (2010) 744–753.
[3] J. Kafaie, R. Song, L. Abrahamyan, A.J. Mouland, M. Laughrea, Virology 375 (2008) 592–610.
[4] M. Mori, L. Kovalenko, S. Lyonnais, D. Antaki, B.E. Torbett, M. Botta, G. Mirambeau, Y. Mély, Curr. Top. Microbiol. Immunol. 389 (2015) 53–92.
[5] H. de Rocquigny, V. Shvadchak, S. Avilov, C.Z. Dong, U. Dietrich, J.L. Darlix, Y. Mély, Mini Rev. Med. Chem. 8 (2008) 24–35.
[6] R.A. Musah, Curr. Top. Med. Chem. 4 (2004) 1605–1622.
[7] C. Abbenhausen, E.J. Peterson, R.E.F. de Paiva, P.P. Corbi, A.L.B. Formiga, Y. Qu, N.P. Farrell, Inorg. Chem. 52 (2013) 11280–11287.
[8] M.A. Castiglione Morelli, A. Ostuni, P.L. Cristinziano, D. Tesauro, A. Bavoso, J. Pept. Sci. 19 (2013) 227–232.
[9] K.P. Bhabak, B.J. Bhuyan, G. Mugesh, Dalton Trans. 40 (2011) 2099–2111.
[10] J.L. Larabee, J.R. Hocker, J.S. Hanas, Chem. Res. Toxicol. 18 (2005) 1943–1954.
[11] K.M. Stuhlmeier, J. Biol. Chem. 282 (2007) 2250–2258.
[12] M.A. Franzman, A.M. Barrios, Inorg. Chem. 47 (2008) 3928–3930.
[13] J.M. Madeira, D.L. Gibson, W.F. Kean, A. Klegeris, Inflammopharmacology 20 (2012) 297–306.
[14] C. Roder, M.J. Thomson, Drugs R. D. 15 (2015) 13–20.
[15] K. Becker, S. Gromer, R.H. Schirmer, S. Müller, Eur. J. Biochem. 267 (2000) 6118–6125.
[16] A. De Luca, C.G. Hartinger, P.J. Dyson, M. Lo Bello, A. Casini, J. Inorg. Biochem. 119 (2013) 38–42.
[17] F. Mendes, M. Groessl, A.A. Nazarov, Y.O. Tsybin, G. Sava, I. Santos, P.J. Dyson, A. Casini, J. Med. Chem. 54 (2011) 2196–2206.
[18] M.G. Lewis, S. DaFonseca, N. Chomont, A.T. Palamara, M. Tardugno, A. Mai, M. Collins, W.L. Wagner, J. Yalley-Ogunro, J. Greenhouse, B. Chirullo, S. Norelli, E. Garaci, A. Savarino, AIDS 25 (2011) 1347–1356.
[19] R.C. Edgar, Nucleic Acids Res. 32 (2004) 1792–1797.
[20] M. Suyama, D. Torrents, P. Bork, Nucleic Acids Res. 34 (Suppl. 2) (2006) W609–W612.
[21] M. Gouy, S. Guindon, O. Gascuel, Mol. Biol. Evol. 27 (2010) 221–224.
[22] D. Darriba, G.L. Taboada, R. Doallo, D. Posada, Nat. Methods 9 (2012) 772.
[23] S. Guindon, O. Gascuel, Syst. Biol. 52 (2003) 696–704.
[24] M. Anisimova, M. Gil, J.F. Dufayard, C. Dessimoz, O. Gascuel, Syst. Biol. 60 (2011) 685–699.
[25] Y. Mély, F. Cornille, M.C. Fournié-Zaluski, J.C. Darlix, B.P. Roques, D. Gerard, Biopolymers 31 (1991) 899–906.
[26] Y. Mély, H. De Rocquigny, N. Morellet, B.P. Roques, D. Gerard, Biochemistry 35 (1996) 5175–5182.
[27] T. Matsui, Y. Kodera, E. Miyauchi, H. Tanaka, H. Endoh, H. Komatsu, T. Tanaka, T. Kohno, T. Maeda, Biochem. Biophys. Res. Commun. 358 (2007) 673–678.
[28] F. Damond, M. Worobey, P. Campa, I. Farfara, G. Colin, S. Matheron, F. Brun-Vezinet, D.L. Robertson, F. Simon, AIDS Res. Hum. Retroviruses 20 (2004) 666–672.
[29] K.A. McCall, C.A. Fierke, Anal. Biochem. 284 (2000) 307–315.
[30] A. Kocyła, A. Pomorski, A. Krężel, J. Inorg. Biochem. 152 (2015) 82–92.
[31] R.W. Alston, L. Urbanikova, J. Sevcik, M. Lasagna, G.D. Reinhart, J.M. Scholtz, C. N. Pace, Biophys. J. 87 (2004) 4037–4047.
[32] D.L. Shapiro, J.R. Masci, J. Rheumatol. 10 (1996) 1818–1820.
[33] T. Okada, B.K. Patterson, S. Ye, M.E. Gurney, Virology 192 (1993) 631–642.
[34] L.R. James, Z.Q. Xu, R. Sluyter, E.L. Hawksworth, C. Kelso, B. Lai, D.J. Paterson, M. D. de Jonge, N.E. Dixon, J.L. Beck, S.F. Ralph, C.T. Dillon, J. Inorg. Biochem. 142 (2015) 28–38.
[35] M.C. Gimeno, in: A. Laguna (Ed.), Modern Supramolecular Gold Chemistry: Gold-Metal Interactions and Application, WILEY-VCH Verlag GmbH & Co. KGaA, Weinheim, 2008, pp. 1–64.
[36] T. Dudev, C. Lim, J. Am. Chem. Soc. 124 (23) (2002) 6759–6766.
[37] E. Bombarda, E. Grell, B.P. Roques, Y. Mély, Biophys. J. 93 (2007) 208–217.
[38] S. Lippard, J.M. Berg, Principles of Bioinorganic Chemistry, University Science Books, Mill Valley, CA, 1994.
[39] Yu-Ming Lee, C. Lim, J. Am. Chem. Soc. 133 (2011) 8691–8703.
[40] A.T. Maynard, M. Huang, W.G. Rice, D.G. Covell, Proc. Natl. Acad. Sci. U.S.A. 95 (1998) 11578–11583.